Quantum coherence and entanglement in the avian compass: Supplementary Material

Erik Gauger,[1] Elisabeth Rieper,[2] John J. L. Morton,[1,3] Simon C. Benjamin,[2,1] and Vlatko Vedral[2,3,4]

[1] *Department of Materials, University of Oxford, Parks Rd, Oxford OX1 3PH, UK*
[2] *Center for Quantum Technologies, National University of Singapore, Singapore*
[3] *Clarendon Laboratory, University of Oxford, Parks Rd, OX1 3PU, UK*
[4] *Department of Physics, National University of Singapore, Republic of Singapore*

(Dated: January 4, 2011)

All principal conclusions of the main paper follow from examining a family of models with the necessary complexity to support the RP mechanism. For brevity, only the most basic model is described in the main paper. We here present several additional calculations and variations of the model, including a variant with more than one nuclear spin, as well as a brief introduction to the terminology used in the main paper.

THE TERMINOLOGY AND TECHNIQUES USED IN THE MANUSCRIPT

The terminology used in the main paper arises from the foundations of quantum mechanics and has more recently become important in the field of quantum information (QI). Thus we describe the avian compass and its dynamics in terms of quantum coherence, environmental decoherence, and entanglement; moreover we use the quantum master equation technique to model the system's dynamics. These terms and techniques are rather different to those of the established radical pair (RP) and avian compass communities, therefore it is appropriate to justify their use and relate them to the established terminology.

The primary conclusion of the paper concerns the extent to which quantum coherence is protected in the compass system. By this term, we refer to the *purity* of the system, which is degraded by interactions with the environment because these will generally act as a kind of measurement of the state (for example, by taking a quantum of energy from the state and thus leaving it in a specific low-energy state). Since the 'outcome' of this measurement is lost to the environment, the system's state becomes a *mixture* of the multiple possible states – generically this loss of purity is called decoherence.

In the applied QI field, much effort is dedicated to the preservation of quantum coherence. In order for quantum coherence to be maintained, it is essential to prevent all kinds of interaction, including those that would *flip* spins, allowing them to relax and lose energy, and also those interactions which would merely alter the *phase* relationships in the state (dephasing noise). Thus while the concept of *spin relaxation* is a typical signature of general coupling to the environment, we must also examine the effect of pure phase noise; the latter alone can suffice to completely degrade a pure state such as the singlet $|s\rangle$ into a completely incoherent mixture of $|s\rangle$ and $|t_0\rangle$ and would therefore undermine our conclusion. In order to examine this point, and establish whether full coherence is indeed maintained, it is necessary to construct a equation for the dynamics of the system where pure phase noise alone occurs. This is most naturally done with the quantum master equation (QME) formalism and the corresponding Lindblad noise operators – however, it is important to note (as mentioned in the main paper) that the QME is actually identical to the more conventional Liouville equation in the case of zero environmental noise. We select the QME as the most suitable tool for examining specific decoherence models, including both general spin relaxation and those that specifically cause only dephasing.

Finally we note that, because the RP involves two electrons, and these are spatially separated, it is meaningful to use the quantity 'entanglement' as one specific characterization of their mutual state. The established avian compass literature would tend to refer to the related concept of *spin correlation*, however, entanglement is subtly and importantly different in that it captures precisely the non-classical correlations between spins – it is impossible, for example, to create entanglement between two sites simply by exchanging classical information as to how the spins should be prepared. We chose to plot the entanglement in the avian compass because it is a key quantity (arguably, *the* essential quantity) in the quantum mechanics, and therefore a reader from that community will naturally wonder about this aspect. However, we find that while entanglement does persist for a remarkably long time, this is likely to be merely an implication of the long coherence time rather than a key property of the compass mechanism.

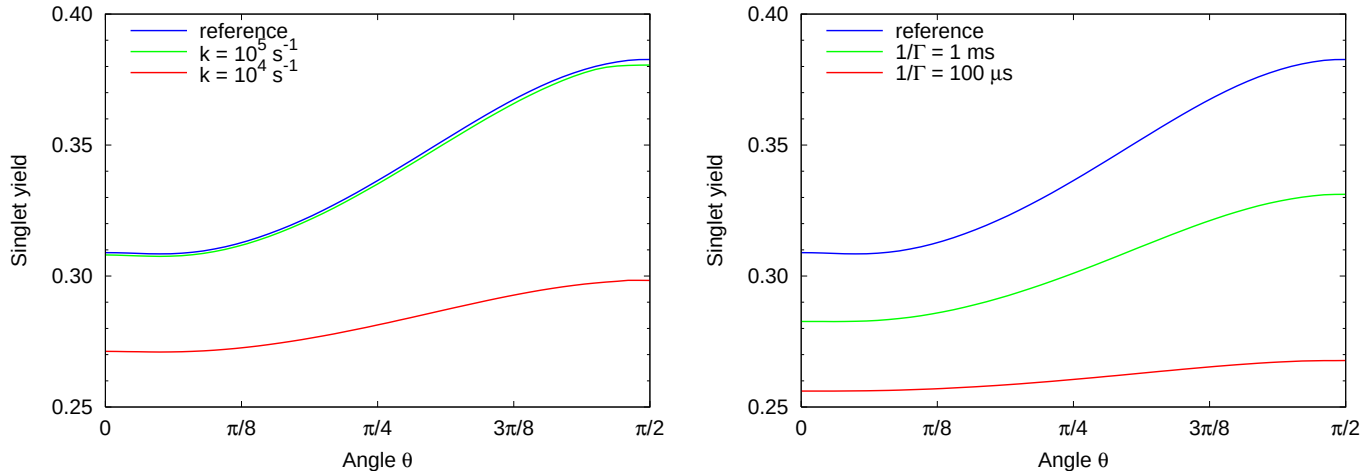

FIG. 1: Results for a disc-shaped HF tensor. The graph on the left is precisely analogous to Fig. 2 of the main text, showing angular dependence of the singlet yield in the presence of the oscillatory field for different decay rates k. The graph on the right corresponds to Fig. 3 of the main paper, showing angular dependence of the singlet yield in the presence of environmental noise [obtained with Eq. (2)] for different noise rates Γ. Although the curve shapes differ, the levels of contrast are the almost the same as the 'cigar' shaped HF model in the main paper.

GENERALITY OF THE MODEL

European robins can adjust to different strengths of the magnetic field. This implies, that their chemical compass cannot depend on the absolute value of the the electron spins hyperfine (HF) coupling. We here argue that the conclusion presented in the main paper is not only robust against variations in the field strength, but also does not depend on the specifics of the anisotropic interaction between electron 1 and its local environment. (Of the two electrons constituting the RP, only one of them can be significantly coupled to nuclear spin(s) because the resonance effect [1] occurs at exactly the frequency of the Zeeman splitting of an *unperturbed* electron.)

'Disc-shaped hyperfine tensor'

We have explicitly checked that our conclusions do not rely on the specifics of the HF tensor given in the main text. Specifically neither a weaker or stronger coupling, nor a different HF tensor symmetry changes our observations about the shortest time scale required for the process to be sensitive to the oscillatory field. Neither do these factors change the maximal tolerable environmental noise rates to maintain a pronounced signal contrast.

Here we describe one of the variants we have studied: a 'disc-shaped' HF-coupling tensor with coupling strengths that are different from the ones presented in the main paper. The largest coupling here is half as strong as the one presented in the text: $A_x = 0.5 \times 10^{-5}$ meV, $A_y = A_x/6, A_z = A_x$.

Fig. 1 shows that we obtain exactly the same qualitative behaviour as for the parameters used in the main text, the only difference being in the different shape of the singlet yield curve (as expected for a different geometry of HF tensor). The oscillatory field does not have an influence on the singlet yield for $k > 10^4$ s^{-1}, while a noise rate of $\Gamma > 0.1k$ leads to a dramatic reduction of contrast.

Anisotropic g-factor

Instead of coupling to nuclear spin(s), an anisotropic g-factor for one of the electrons could also lead to a singlet yield with an angular dependence [2]. We here show that our main conclusion remains valid under this different Hamiltonian of the RP.

For illustration purposes, we consider a pronounced anisotropy: the g-factor in z-direction is 0.8×2, i.e. 80% of the free electronic g-factor of $g = 2$, while in x and y-direction we have 0.3×2. A smaller anisotropy works as well,

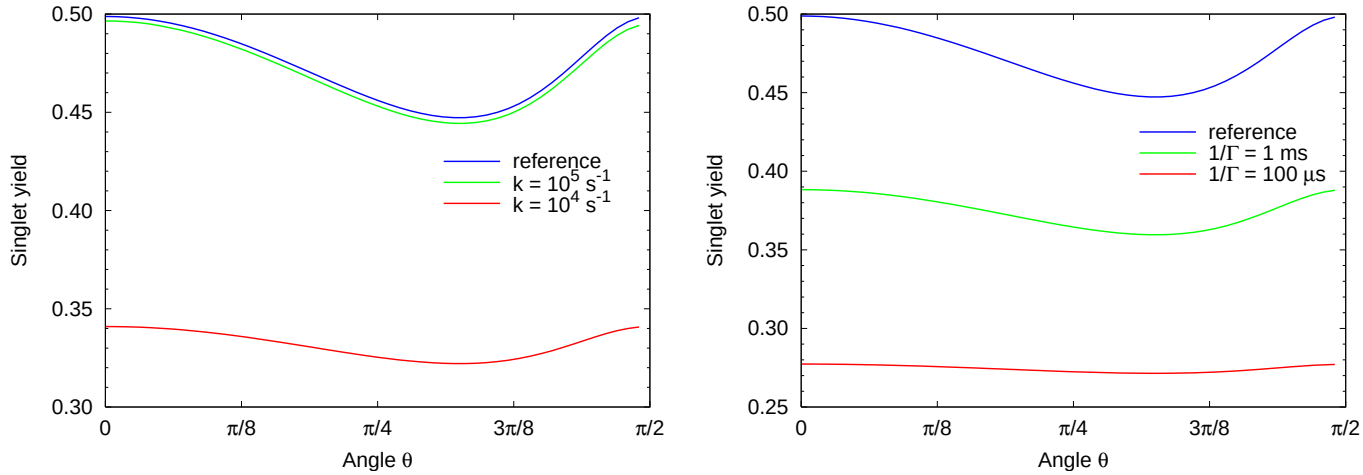

FIG. 2: Results for a model in which an anisotropic g-factor replaces the role of the nucleus to break the RP symmetry. The graph on the left is precisely analogous to Fig. 2 of the main text, showing angular dependence of the singlet yield in the presence of the oscillatory field for different decay rates k. The graph on the right corresponds to Fig. 3 of the main paper, showing angular dependence of the singlet yield in the presence of environmental noise for different noise rates Γ. Although the curve shapes differ, remarkably the levels of contrast remain similar to those of the conventional model in the main paper.

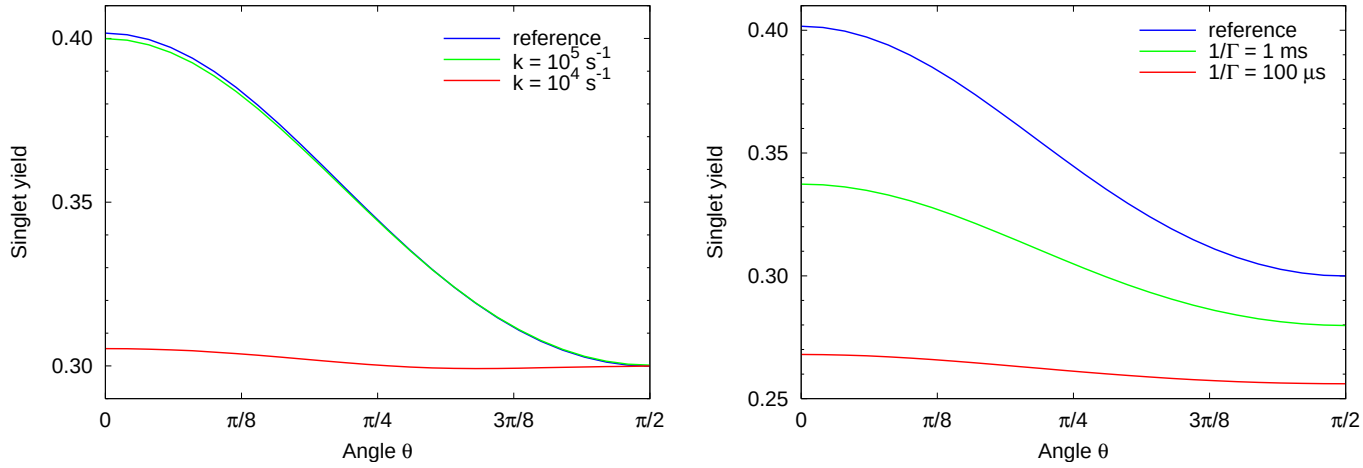

FIG. 3: Results for two nuclear spins coupled to electron 1. The graph on the left is precisely analogous to Fig. 2 of the main text, showing angular dependence of the singlet yield in the presence of the oscillatory field for different decay rates k. The graph on the right corresponds to Fig. 3 of the main paper, showing angular dependence of the singlet yield in the presence of environmental noise for different noise rates Γ. Although the curve shapes differ somewhat, nevertheless the parameters corresponding to serve degradation remain the same as those in the main paper ($k = 10^4$ s^{-1}, $\Gamma = 100$ μs).

but gives less overall signal contrast (even in the unperturbed) scenario. We present results for these parameters in Fig. 2, confirming that the qualitative behaviour is still the same under these assumptions.

RP pair model with two nuclear spins

In the model described in the main paper, there is a single nuclear spin coupled to one of the electrons. However, previous publications have studied the case where more than one nuclear spin is present [1, 3, 4]. Therefore, it is interesting to check whether the addition of a nuclear spin will alter our conclusions. The Hamiltonian now gains an additional coupling term,

$$H = \hat{I}_1 \cdot \mathbf{A}_1 \cdot \hat{S}_1 + \hat{I}_2 \cdot \mathbf{A}_2 \cdot \hat{S}_1 + \gamma \mathbf{B} \cdot (\hat{S}_1 + \hat{S}_2),$$

where $\mathbf{A}_1$ is the HF tensor of the main text and $\mathbf{A}_2 = 2/3\mathbf{A}_1$. Here we choose a second rugby shaped HF tensor oriented parallel to the first. Note that we have also considered different relative coupling strengths and geometries (such as a pancake shaped and rugby shaped tensor), but again, these choices do not influence our core conclusions. Results for the particular choice of parameters described above are shown in Fig. 3.

PURE DEPHASING NOISE MODEL

Interestingly, if we begin the simulation with a completely dephased state: $(|s\rangle\langle s| + |t_0\rangle\langle t_0|)/2$, the classical correlations are still sufficient for achieving adequate angular visibility and neither quantum phase coherence nor entanglement seems to be a prerequisite for the efficiency of the avian compass.

To explore this idea further, we would like to study 'pure dephasing' occurring *during* the singlet-triplet interconversion. In essence we use energy conserving noise operators, Eqn. (1), which are known to be the dominant source of decoherence in so many other artificially made quantum systems. By applying this specific noise, we confirm that the compass mechanism's performance is essentially immune, while of course the coherence of the quantum state of the electrons would be degraded.

One might be inclined to conclude that, if pure dephasing noise is indeed dominant, then the avian compass need not protect quantum coherence for the long time scales suggested in the main paper. But crucially, we also show that if such noise were naturally present at a high level in the compass (exceeding the generic noise level Γ by more than an order of magnitude) then it would render the bird immune to the weak oscillatory magnetic fields studied by Ritz *et al.* [1]. Thus the sensitivity to oscillatory fields implies that both amplitude and phase, and thus entanglement, are indeed protected within the avian compass on timescales exceeding tens of microseconds.

Since the electron spin singlet state is not an eigenstate of the Hamiltonian, the dephasing operators will be different from the ones mixing the phase of the singlet and triplet state within the electronic subspace. Instead, we replace the previously defined noise operators of L_i of Eq. (3) by appropriate dephasing operators as follows: we treat the remote electron and the electron nuclear spin subsystem separately. Within both subsystems, we define dephasing operators

$$Z_i = \frac{1}{\sqrt{2}} \left(\sum_{j \neq i} |\lambda_j\rangle\langle\lambda_j| - |\lambda_i\rangle\langle\lambda_i| \right) = \frac{1}{\sqrt{2}} \left(I_4 - 2|\lambda_i\rangle\langle\lambda_i| \right), \tag{1}$$

where $\{|\lambda_i\rangle\}$ are the set of normalised eigenvectors of this subsystem. This results in two dephasing operators for the remote electron (these can be combined to a single σ_z operator rotated with the field) and four operators for the electron nuclear spin subsystem. Each of these dephasing operators corresponds to fluctuations of one of the (subsystem's) energy levels.

Strikingly, the singlet yield is entirely unaffected by this particular kind of noise, i.e. it is entirely independent of the dephasing rate Γ_z. Thus, a curve obtained with this model coincides perfectly with the reference curve of Fig. 3 of the main paper. However, we show in the following that the dephasing rate of this model can be at most ten times faster than the generic noise rate to retain sensitivity to the oscillatory field.

Fig. 4 shows the singlet yield as a function of θ for different pure dephasing rates Γ_z. Pure phase noise would actually *protect* the compass from the harmful effect of an applied oscillatory field (by suppressing the Rabi oscillations caused by such a field). We see that an aggressive pure dephasing rate of $1/\Gamma_z = 10$ μs almost completely recovers the reference curve (corresponding to a noise-free system without oscillatory field).

OSCILLATORY FIELD SENSITIVITY IN THE PRESENCE OF NOISE

In the first stage of the argument in the main paper, we show how the bird's sensitivity to field angle is degraded by an applied oscillatory field (Fig. 2, main paper). There we set the environmental noise operators to zero – this is of course unrealistic, and one might worry that finite noise could ultimately lead to less dramatic conclusions regarding protection of quantum coherence. However, here we show that the reverse is true: the addition of finite noise leads to a suppression of the harmful effect of the oscillatory field, and thus would lead one to infer a still more dramatic coherence time. Therefore, by setting the noise to zero we make the more conservative assumption.

We confirm this by employing the following master equation (which is exactly Eq. (3) of the main paper), while at

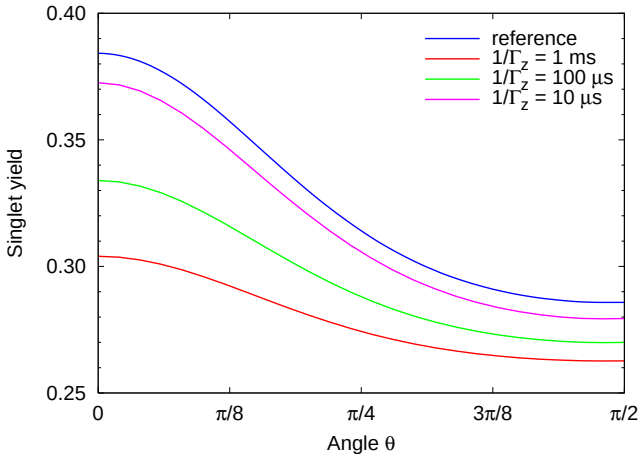

FIG. 4: Angular dependence of the singlet yield at $k = 10^4$ s^{-1} in the presence of the oscillatory field for different pure dephasing rates Γ_z. This is to be compared with the $k = 10^4$ s^{-1} line in Fig. 2 of the main paper. See text for an explanation.

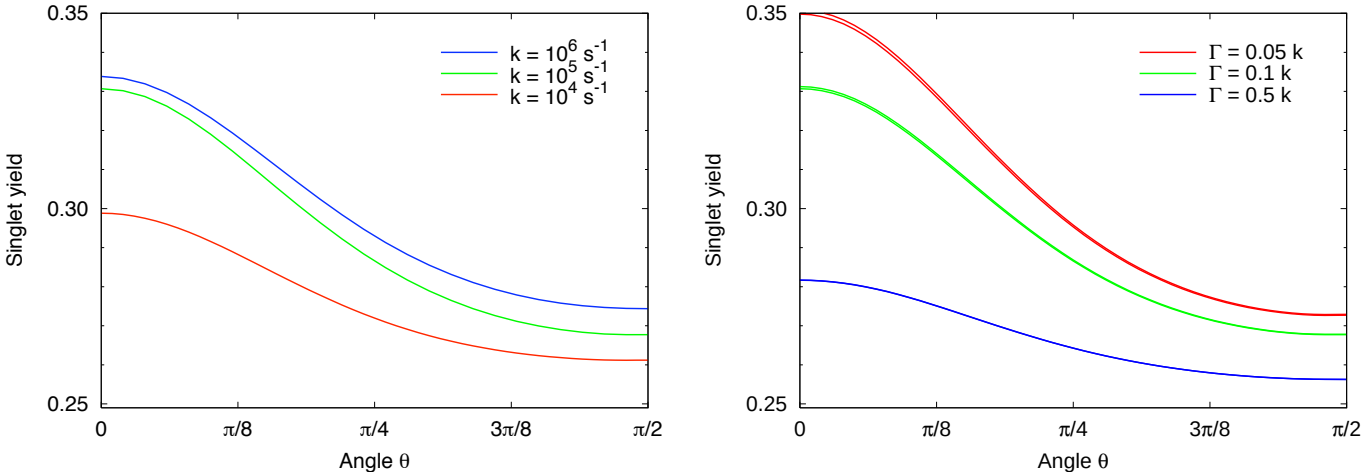

FIG. 5: **Left:** singlet yield as a function of θ in the presence of the resonant oscillatory field with additionally applied noise at a rate $\Gamma = 0.1k$ (see text). **Right:** The singlet yield as a function of θ, this time with k fixed at $k = 10^5$ s^{-1} and for different noise rates. For each noise rate, there are two curves, one with and one without the oscillatory field. However, as explained in the text, these can only be properly distinguished for the case of weak noise (red curves).

the same time applying the oscillatory field:

$$\dot{\rho} = -\frac{i}{\hbar}[H,\rho] + k\left(\sum_{i=1}^{8} P_i\rho P_i^\dagger - \frac{1}{2}\left(P_i^\dagger P_i\rho + \rho P_i^\dagger P_i\right)\right) + \sum_{i=1}^{6}\Gamma_i\left(L_i\rho L_i^\dagger - \frac{1}{2}\left(L_i^\dagger L_i\rho + \rho L_i^\dagger L_i\right)\right). \tag{2}$$

The left panel of Fig. 5 corresponds to Fig. 2 of the main paper with such *additionally* applied noise at a rate of $\Gamma = 0.1k$. Note that the noise rate is adjusted with k, as we wish to concentrate on the combined effect of the oscillatory field and 'mild noise' over the timescale of the process. We infer that the singlet yield contrast is only significantly reduced when $k < 10^5$ s^{-1}, meaning the addition of noise to Fig. 2 in the main paper does not influence our conclusion.

To establish that this conclusion is robust with respect to the particular choice of $\Gamma = 0.1k$, we now investigate *different* noise rates for a fixed value of $k = 10^5$ s^{-1}. In the right panel of Fig. 5, we show a pair of curves for each noise rate: one obtained with and one without the oscillatory field. We make two observations: firstly, the two curves of each pair nearly coincide, indicating that there is only a small sensitivity to the oscillatory field independent of the noise rate. Secondly, the sensitivity *decreases* even more when the system is subjected to more aggressive noise.

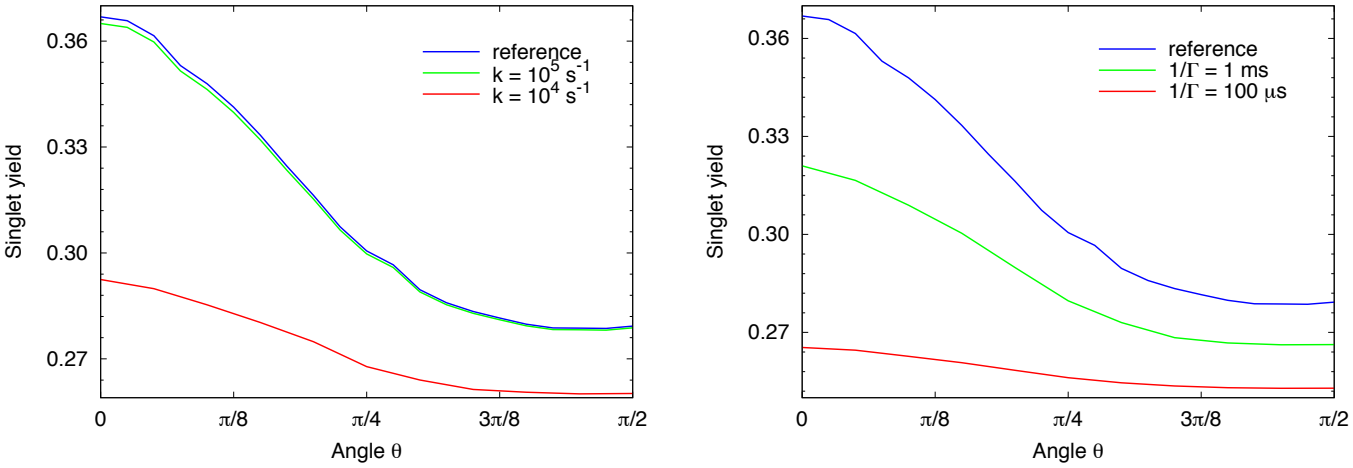

FIG. 6: Results for an additional nuclear spin bath interacting with electron 1. The graph on the left is precisely analogous to Fig. 2 of the main text, showing angular dependence of the singlet yield in the presence of the oscillatory field for different decay rates k. The graph on the right corresponds to Fig. 3 of the main paper, showing angular dependence of the singlet yield in the presence of environmental noise for different Markovian noise rates Γ.

In fact, this second observation is not surprising: we would not expect the additional noise terms to lead to a greater sensitivity to the oscillatory field. The singlet yield signal is corrupted by spin flips of the remote electron in the presence of the oscillatory field, which essentially causes the spin to Rabi flop, thus requiring quantum coherence. Therefore, any noise acting on the remote electron will decohere the spin and thus suppress rather than enhance the effect of the oscillatory field. This can also be seen in the right panel of Fig. 5: the red curves are very similar but not quite identical, the agreement is better for the green curves and almost perfect for the blue one.

NON-MARKOVIAN NOISE

The noise model discussed in the main paper is Markovian, implying that the information lost to the environment will not return to the system (as it would, wholly or partially, if the environment was entirely constituted by other isolated qubits that could effectively act as a memory). This Markovian assumption is the natural choice to make for a room temperature system whose detailed structure and environmental interactions are unknown. One can immediately think of 'likely suspects' for decoherence in the present system that would be Markovian: for example, modulation in the electron-electron separation due to vibrations in the supporting matrix.

While one can reasonably speculate that there may *also* be non-Markovian processes occurring, between the core system and other degrees of freedom that are well isolated from the true 'bath' degrees of freedom, this does not undermine our result. In essence, one would 'draw a dotted line' around the larger system, comprised of the core electron pair *together* with the non-Markovian environment, calling *that* the avian compass (although noting that only the core part plays an active role). One would conclude that this larger system is, again, remarkably well insulated from the environment. The protection of quantum coherence in such a larger system could be considered to be even more remarkable, since one would expect a larger and more complex system to be more rather than less susceptible to environmental fluctuations.

In the following, we shall provide a more quantitative discussion of non-Markovian noise. Essentially, non-Markovian processes can affect the quantum evolution of a quantum system in two distinct ways: if the local environment only features a small number of degrees of freedom that serve as a quantum memory, quantum coherence is preserved and can be channelled back into the system. On the other hand, a larger non-Markovian environment is typically manifested by a non-exponential but irreversible decay of the coherences (e.g. 1/f noise). However, in this latter case, the implications are exactly the same as those deduced from our Markovian noise model: the compass is only susceptible to the oscillatory field as long as its electron spins retains their quantum coherence, and the precise profile of any irreversible loss of coherence is thus immaterial. Therefore, the interesting case to study is that of a smaller local spin bath, where the dynamics of the combined compass and spin bath follow a pure evolution. After tracing over the additional nuclear spins, the reduced dynamics of the RP spins is then non-Markovian. However, as described

above with the 'dotted line picture' some level of Markovian noise will also be inevitably present on the long timescale required for the RP process, thus we are still dealing with a computationally demanding open systems problem, limiting the number of spins that can be simulated.

Figure 6 shows results obtained for a RP model consisting of two electron and four nuclear spins. As before, one of the nuclear spins is a central part of the mechanism through its anisotropic coupling to electron 1 with parameters as in the main paper. The remaining three nuclear spins serve as an additional local spin bath, and we have assumed isotropic hyperfine coupling strengths of $A2 = A_z/8,\ A3 = A_z/10,\ A3 = A_z/12$ with electron 1 ($A_z = 10^{-5}$ meV). All nuclear spins are initialised in a fully mixed state as appropriate for a room temperature environment. The presence of the additional nuclear spins introduces some ripples into the shape of the curves, yet there is no qualitative difference with regard to the effects of irreversible noise and the oscillatory field. This means that we must once more arrive at the same conclusion that the compass system is remarkably well protected from an irreversible loss of coherence. We note that further calculations with only three protons and for a range of different coupling strengths (not shown) display the same qualitative behaviour, indicating that there is no trend for an increasing number of spins that would alter our conclusion.

ADDITIONAL NOISE MODELS

While the noise model covered in the main paper is the most natural assumption to make for a biological system at high temperature, we will in the following explore whether more exotic forms of correlated noise would allow us to escape the conclusion of the extraordinarily long coherence time. To distinguish the isotropic noise model of the main paper from the ones discussed here, we shall refer to it as 'general noise' in the following.

The basic RP model consists of three spins and hence there exist 64 combinations of the form $L = S_i \otimes S_j \otimes S_l$ for $S_{i,j,l} \in \{I_2, \sigma_x, \sigma_y, \sigma_z\}$. The identity, I_2, on all three spins does not lead to decoherence, so that there are 63 effective Lindblad operators in this 8-dimensional Hilbert space. As a first step we examine the action of all 63 processes (added incoherently) with equal weighting acting simultaneously. As a variant, we also consider those 15 Lindblad operators from the set of the 63 which do not affect the nuclear spin, motivated by the fact that the nuclear spin is initialised in a fully mixed state and its coherence plays no crucial role in the functioning of the compass.

Fig. 7 shows the results for the model of 63 and 15 Lindblad operators compared to the general noise model from the main paper. After appropriately scaling the noise rate associated with each of the noise processes (instead of the six independent processes in the general noise model, there are now 63 or 15, respectively), we see that there is very little difference to the general noise model. Furthermore, there is no qualitative difference between the model which includes noise on the nuclear spin and the one that does not.

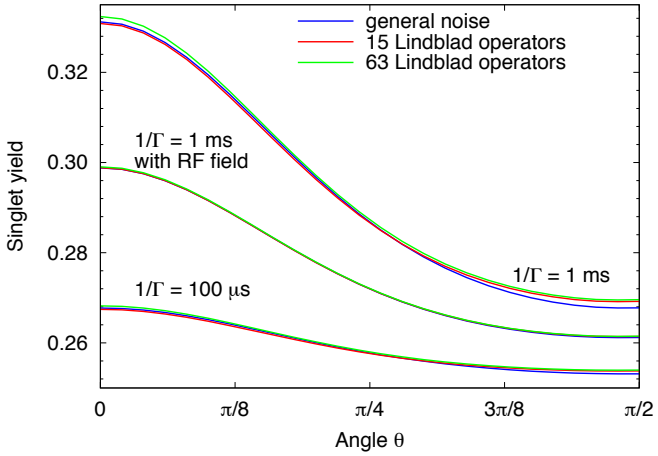

FIG. 7: Comparison of the general noise model from the paper and the models with 63 and 15 Lindblad operators. The noise rate for each individual Lindblad operator is scaled by 6/63 and 6/15, respectively, to account for the increased aggressiveness due to a larger number of noise processes. For a coherence time of 1 ms there is still a significant decrease of singlet yield when the RF field is applied. The curves with RF field for a coherence time of 100 μs are not shown since their downwards shift is very small and they heavily overlap with the lower bundle of curves in the figure.

Having simultaneously considered all 63 processes, we now look at the effect of individual Lindblad operators. We focus on the nine subsets of operators which affect coherence on *both* electron spins (otherwise the coherence time of at least one part of the compass would be infinite). Summing over the four possible nuclear combinations, we obtain the manageable number of nine noise models, each with isotropic noise on the nuclear spin [5].

All curves in our calculations have the same shape with the largest singlet yield achieved for $\theta = 0$ and the lowest singlet yield in the perpendicular configuration $\theta = \pi/2$. The difference in singlet yield between those two configurations corresponds to the signal contrast and is a good measure for judging the performance of the compass. In the absence of noise and the oscillatory field, the contrast is $0.382 - 0.281 = 0.101$, and we shall use this value as the benchmark for comparing the different noise models.

Noise model	**Noise [%]**	**Noise & RF [%]**	**Degradation [%]**	**Noise [%]**	**Noise & RF [%]**	**Degradation [%]**
	$1/\Gamma = 100$ μs			$1/\Gamma = 10$ μs		
general noise	14.49	13.98	3.54	1.65	1.649	0.05
$\sigma_x \otimes \sigma_x$	39.09	34.55	11.62	5.85	5.83	0.23
$\sigma_x \otimes \sigma_y$	40.45	35.78	11.55	6.05	6.03	0.23
$\sigma_x \otimes \sigma_z$	12.72	11.61	8.73	1.42	1.41	0.16
$\sigma_y \otimes \sigma_x$	40.45	35.82	11.46	6.05	6.03	0.23
$\sigma_y \otimes \sigma_y$	39.09	34.59	11.51	5.84	5.83	0.23
$\sigma_y \otimes \sigma_z$	11.36	10.42	8.26	1.21	1.21	0.16
$\sigma_z \otimes \sigma_x$	12.72	12.24	3.77	1.42	1.42	0.05
$\sigma_z \otimes \sigma_y$	11.36	11.02	3.02	1.21	1.21	0.03
$\sigma_z \otimes \sigma_z$	39.09	35.98	7.97	5.84	5.83	0.15
pure dephasing	99.999	63.45	36.55	99.991	92.41	7.58
match experiment	high	strongly reduced	high	high	strongly reduced	high

TABLE I: Contrast for the nine different Lindblad operators compared to the isotropic noise model of the main paper and the pure dephasing noise. The "Noise model" column specifies the type of noise and for the $\sigma_i \otimes \sigma_j$ entries σ_i and σ_i are the noise acting on the 'local' and 'remote' electron spin respectively. The "Noise" and "Noise & RF" columns give the signal contrast as a percentage of the ideal unperturbed system (see text). The "Degradation" columns show the percent decrease of signal contrast when the oscillatory radio frequency field is applied. To be consistent with experimental data, the signal contrast without RF field should be sufficiently large, and it should decrease significantly when the oscillatory field is applied. The last row is added for ease of checking the consistency of a particular noise model with the experimental data.

The results of this calculation are presented in Table I. Recall that the assertion in the main paper is that the quantum coherence time in the compass must exceed 100 μs given the 'general noise' model, while for the most permissive model we could find – the 'pure dephasing' model – the time must still exceed 10 μs. The extended statement we can now make is the following: None of the noise models considered in the table can lead to coherence times of $10\mu s$ or less; the behaviour of the nine new models lies between the 'general noise' and the 'pure dephasing' but is closer to the former. The righthand triplet of columns show that setting $\Gamma = 10$ μs leads to mismatch with experimental data for all models. As expected the 'pure dephasing' model performs best, and permits the compass to function as if no noise were present. However even this model cannot account for the fact that weak a RF field completely disrupts the compass, since the model predicts only a 7.58% reduction in contrast under such a field (a small modulation given that birds can adapt to different static field strengths, which leads to natural variations in the magnitude and of the singlet yield). Moreover, from the lefthand triplet of columns, we notice that only the 'pure dephasing' model can provide plausible fit to data even for $\Gamma = 100$ μs. The other new models considered here cannot do so: some of the nine noise models display a similar performance to 'general noise' while others perform slightly better.

In summary, our results show conclusively that the pure dephasing represents the most extreme case of all the models considered here, requiring a coherence time of more than 10 μs, whereas all other types of noise need to preserve quantum coherence longer in order to be consistent with experimental data.

[1] T. Ritz et al.: *Magnetic Compass of Birds Is Based on a Molecule with Optimal Directional Sensitivity*, Biophysical Journal, **96** 3451-3457, (2009).

[2] I.A. Solov'yov, D. E. Chandler, K. Schulten:*Magnetic Field Effects in Arabidopsis thaliana Cryptochrome-1*, Biophysical Journal, **92**, 2711-2726 (2007).
[3] C. T. Rodgers, P.J. Hore: *Chemical magnetoreception in birds: The radical pair mechanism*, PNAS, **106** 2, 353-360, (2009).
[4] C.T. Rodgers:*Magnetic Field Effects in Chemical Systems*, PhD Thesis, Oxford (2007).
[5] As further variants, we have also checked a small number of models with the identity or another specific noise operator acting on the nuclear spin. However, the results were entirely in line with the rest of the discussion, i.e. we found no combination that would be consistent with the experimental data.